

Combining Effective Hamiltonians and Brillouin-Wigner Approach: A Perturbative Approach to Spectroscopy

Oussama Bindech

Laboratoire de Chimie Quantique, Institut de Chimie, CNRS/Université de Strasbourg, 4 rue Blaise Pascal, 67000 Strasbourg, France

Bastien Valentin

Laboratoire de Chimie Quantique, Institut de Chimie, CNRS/Université de Strasbourg, 4 rue Blaise Pascal, 67000 Strasbourg, France

Saad Yalouz*

E-mail: syalouz@unistra.fr

Laboratoire de Chimie Quantique, Institut de Chimie, CNRS/Université de Strasbourg, 4 rue Blaise Pascal, 67000 Strasbourg, France

Vincent Robert*

E-mail: vrobert@unistra.fr

Laboratoire de Chimie Quantique, Institut de Chimie, CNRS/Université de Strasbourg, 4 rue Blaise Pascal, 67000 Strasbourg, France

Abstract. The numerical cost of variational methods suggests using perturbative approaches to determine the electronic structure of molecular systems. In this work, a sequential construction of effective Hamiltonians drives the definition of approximate model functions and energies in a multi-state Rayleigh-Schrödinger perturbative scheme. A second step takes advantage of an updated partitioning of the Hamiltonian to perform a state-specific Brillouin-Wigner energy correction based on a well-tempered perturbation expansion. The multi-step RSBW method is exemplified on model-Hamiltonians to stress its robustness, efficiency and applicability to spectroscopy determination.

1. Introduction

A key point in the study of strongly correlated systems is selecting a computational method that can balance computational feasibility with a high-level description of many-electron effects. To achieve spectroscopic accuracy, a Full Configuration Interaction (FCI) expansion of the wavefunction is theoretically the most precise option possible. While many recent works have focused on developing variants and extensions of this approach (see, for example, Refs. [1–7]), FCI-like methods remain computationally prohibitive due to their exponential numerical cost, prompting the search for alternative approaches. One such alternative is the Complete-Active-Space Self-Consistent Field (CASSCF) approach [8–10], which leverages a Complete Active Space (CAS) wavefunction expansion combined with orbital optimization techniques. In practice, this method is considered a reference tool for capturing most of the so-called “static correlation”, inspiring numerous recent developments focused on orbital optimization. [11–20] However, even within such methods, achieving spectroscopic accuracy remains a key issue due to the missing electronic “dynamical” correlation contributions. To address this, perturbative treatments offer a systematic order-by-order expansion to introduce the missing contributions. In perturbative theory, the exact Hamiltonian \hat{H} is divided into a reference \hat{H}_0 and a perturbation \hat{W}_0 , such that $\hat{H} = \hat{H}_0 + \hat{W}_0$. The success of this approach depends on \hat{H}_0 's ability to produce accurate reference eigenstates and eigenvalues. Practically, \hat{H}_0 must include the dominant contributions while remaining simple enough to be computationally tractable. Challenges, however, may arise due to quasi-degenerate states, which can lead to vanishing energy denominators and divergence in the expansion series. Besides, the presence of so-called intruder states can also be problematic in a Complete Active Space Second-Order Perturbation Theory treatment. [21, 22] This issue can be elegantly mitigated by using the N-electron Valence State Perturbation Theory (NEVPT2). [23–25]

The leading perturbative methods rely on Brillouin-Wigner (BW) or Rayleigh-Schrödinger (RS) schemes. [26–30] In both approaches, the splitting and related definition of the model (e.g., active space) and orthogonal (so-called perturbers) spaces might not be straightforward. While the former does not suffer from the intruder states issue, it is much less widely

used, possibly because of the energy-dependent structure of the energy expansion and the size-extensivity error. [31] Despite this, the systematic order-by-order expansion to achieve state-specific energy corrections makes it very appealing.

The Epstein-Nesbet partition, a variant of the RS approach with a zero-diagonal perturbation, [32, 33] has proven to be limited when states are expressed as linear combinations of non-degenerate configurations. A significant improvement was brought by the Configuration Interaction using a Perturbative Selection done Iteratively (CIPSI) method. It is to be considered as a landmark in RS expansions when multiconfigurational wavefunction are necessary. [34]

More recently, the combination of RS and BW theories has provided an original two-step method (referred to as RSBW) to progressively include perturbation effects. [35] The RSBW procedure follows the reconstruction of the zeroth-order Hamiltonian from the effective Hamiltonian diagonalization, thereby implementing part of the perturbation effects in the subsequent BW expansion. Even though the relevance of the method was evaluated, the re-partitioning of the Hamiltonian may not be systematic enough to guarantee an improved convergence in the BW energy expansion. A prerequisite in the RSBW method is a clear-cut definition of the model space to construct and diagonalize an effective Hamiltonian.

In this work, we propose an extension of the RSBW method using a multi-step approach to identify the configuration subspaces that necessitate RS treatment. The method employs a scanning procedure across the spectrum by constructing successive effective Hamiltonians. This approach enables (i) accounting for static correlation effects and (ii) progressively mitigating the influence of the updated perturbation on the redefinition of the zeroth-order Hamiltonian. In the final step, a state-specific BW energy expansion is conducted to deliver a perturbative approach to the spectroscopy of model systems. This method can be considered as an alternative to demanding full diagonalization, leveraging the individual strengths of the RS and BW approaches.

In a first section of this paper, an overview of the previously reported RSBW method is given to stress its limitation and to motivate the multi-step RSBW extension. Then, the method is applied to parameterized Hamiltonians.

2. Construction of a well-tempered perturbation expansion.

2.1. RSBW method: an overview

Recently, a two-step perturbative approach has been proposed by taking advantage of the RS and BW schemes. [35] The RSBW method starts with the definition of an appropriate model space P constructed on model configurations $\{|\alpha\rangle\}$, which are eigenfunctions of the unperturbed Hamiltonian \hat{H}_0 [36]:

$$\hat{H}_0|\alpha\rangle = \mathcal{E}_\alpha|\alpha\rangle. \quad (1)$$

The diagonalization of the second-order effective Hamiltonian in the P -space produces model functions $\{|\Psi_\alpha^{\text{RS}}\rangle\}$, energies $\{E_\alpha^{\text{RS}}\}$, and a different partitioning $\hat{H} = \hat{H}^{\text{RS}} + \hat{W}$ with

$$\hat{H}^{\text{RS}} = \sum_{\alpha \in P} E_\alpha^{\text{RS}} |\Psi_\alpha^{\text{RS}}\rangle \langle \Psi_\alpha^{\text{RS}}| + \sum_{\beta \in Q} E_\beta^{\text{RS}} |\beta\rangle \langle \beta|. \quad (2)$$

The so-called perturbers $\{|\beta\rangle\}$ with energies $E_\beta^{\text{RS}} = \mathcal{E}_\beta = \langle \beta | \hat{H}_0 | \beta \rangle$ span the orthogonal Q -space. The impact of $\hat{W} = \hat{H} - \hat{H}^{\text{RS}}$ is reduced as compared to that of $\hat{W}_0 = \hat{H} - \hat{H}_0$ since part of the perturbation contributions are included in the effective Hamiltonian: this is the essence of the RSBW method. The missing contributions are then included in a truncated BW energy expansion where the exact energy E_i^{exact} is approximated as E_i^{RSBW} and the energy denominators are set to $E_i^{\text{RSBW}} - E_j^{\text{RS}}$ in the m^{th} order expansion of the resolvent:

$$\hat{\Omega}_i^{(m)} = \left(\sum_{j \neq i} \frac{|\Psi_j\rangle \langle \Psi_j|}{E_i^{\text{exact}} - \hat{H}^{\text{RS}}} \hat{W} \right)^m. \quad (3)$$

Despite its performance reflected by an improved convergence, the RSBW method relies on the identification of a convenient model space which remains a bottleneck (intruder state issue). Thus, we considered that such limitation could be overcome by a systematic screening of the states energies and couplings, to step-by-step build and diagonalize effective Hamiltonians before applying a final BW treatment.

2.2. Multi-step RSBW method

Starting from the ground state energy \mathcal{E}_0 of \hat{H}_0 , a screening of the zeroth-order eigenenergies $\{\mathcal{E}_\gamma\}$ is performed through the evaluation of the ratios

$$\rho_{0\gamma,1} = \left| \frac{\langle 0 | \hat{W}_0 | \gamma \rangle}{\mathcal{E}_0 - \mathcal{E}_\gamma} \right|, \quad (4)$$

where $|0\rangle$ and $|\gamma\rangle$ are the corresponding eigenvectors, and the extra index refers to the first RS transformation. The objective is to identify the $|\gamma\rangle$'s that

fulfill $\rho_{0\gamma,1} > \rho_{\text{min}}$, with ρ_{min} an arbitrary threshold value. Such criterion emerging from perturbation theory in quantum mechanics is the guiding one for the progressive sub-space definition in the CIPSI method. [34] This procedure makes it possible to develop a model space P_1 based on a perturbation criterion. Evidently, the smaller the ρ_{min} value, the larger the dimension d_1 of the P_1 -space, and strictly degenerate states (*i.e.* $\mathcal{E}_\gamma = \mathcal{E}_0$) are automatically retained following the Bloch theory. If the P_1 -space dimension is unity after this procedure ($d_1 = 1$), a similar screening is conducted from \mathcal{E}_1 , and possibly from higher-lying eigenstates of \hat{H}_0 , until a model space with $d_1 \geq 2$ is identified. The states which do not belong to P_1 are referred to as perturbers $|\beta\rangle$. Where this condition is not met, one would be tempted either to use standard perturbation theory, or to reduce the threshold value ρ_{min} . In practice, challenging issues stem from quasi-degenerate states in some energy windows (*e.g.* singlet-triplet energy difference in the low-energy spectrum). Therefore, the screening effort might be rather limited to concentrate on a selection of states with the identification of possible intruders in the \hat{H}_0 spectrum. Following the RSBW method, (*i*) a second-order effective Hamiltonian is built and diagonalized in the identified model space P_1 , and (*ii*) an updated zeroth-order Hamiltonian \hat{H}_1^{RS} (see Eq. 2) and perturbation \hat{W}_1 are defined.

This procedure is then repeated as shown in Figure 1 (restricted to two steps for illustration). In the following, we shall use the notations $\{E_{i,n}^{\text{RS}}\}$ and $\{E_{i,n}^{\text{RSBW}}\}$ to refer to the approximate eigenenergies obtained from the RS and the RSBW treatments, respectively. In this labelling, the index i is used to reference the approximate eigenstates $\{|\Psi_{i,n}^{\text{RS}}\rangle\}$ of the system and n refers to the number of RS steps. At step $n+1$, the screening is performed from the partitioning $\hat{H} = \hat{H}_n^{\text{RS}} + \hat{W}_n$ with the RS Hamiltonian

$$\hat{H}_n^{\text{RS}} = \sum_{\alpha \in P_n} E_{\alpha,n}^{\text{RS}} |\Psi_{\alpha,n}^{\text{RS}}\rangle \langle \Psi_{\alpha,n}^{\text{RS}}| + \sum_{\beta \in Q_n} E_{\beta,n}^{\text{RS}} |\Psi_{\beta,n}^{\text{RS}}\rangle \langle \Psi_{\beta,n}^{\text{RS}}| \quad (5)$$

(with $\hat{H}_0^{\text{RS}} = \hat{H}_0$) to generate the next P_{n+1} - and Q_{n+1} -spaces under the condition:

$$\rho_{ij,n+1} = \left| \frac{\langle \Psi_{i,n}^{\text{RS}} | \hat{W}_n | \Psi_{j,n}^{\text{RS}} \rangle}{E_{i,n}^{\text{RS}} - E_{j,n}^{\text{RS}}} \right| > \rho_{\text{min}}. \quad (6)$$

In all notations, the extra lower index n indicates the number of performed RS transformations. Since the diagonalization is restricted to the P_{n+1} model space, the orthogonal Q_{n+1} states energies (*i.e.* the perturbers $|\Psi_{\beta,n}^{\text{RS}}\rangle$ energies) remain identical to the ones at step n , $E_{\beta,n+1}^{\text{RS}} = E_{\beta,n}^{\text{RS}} = \langle \Psi_{\beta,n}^{\text{RS}} | \hat{H}_n^{\text{RS}} | \Psi_{\beta,n}^{\text{RS}} \rangle$. Two important points should be made regarding the strategy. First, the ρ_{min} value directly controls the size

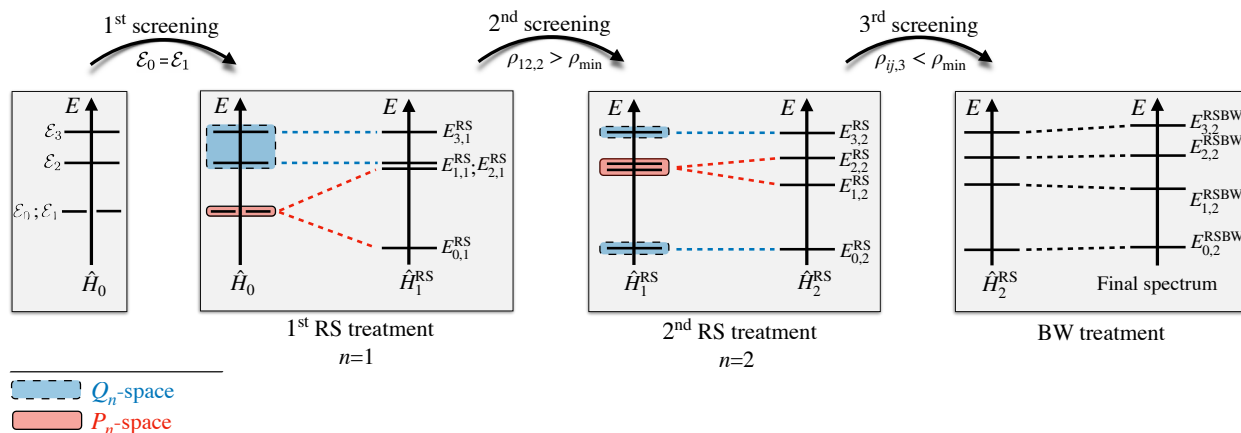


Figure 1: Description of the multi-step RSBW method. For the sake of simplicity, only two steps are shown. The first one uses a $\hat{H} = \hat{H}_0 + \hat{W}_0$ partitioning, whereas the second step takes advantage of the redefinition of the zeroth-order Hamiltonian following the RSBW strategy $\hat{H} = \hat{H}_1^{\text{RS}} + \hat{W}_1$. At each step n , the screening procedure identifies the $|\Psi_{j,n}^{\text{RS}}\rangle$ states that for a given $|\Psi_{i,n}^{\text{RS}}\rangle$ state are either strictly degenerate or fulfill $\rho_{ij,n} > \rho_{\min}$ to build up the P_n and Q_n spaces. In the final step, the eigenstates and eigenenergies of \hat{H}_2^{RS} provide an improved zeroth-order states and zeroth-order energies of the system perturbed by \hat{W}_2 used for the final BW treatment.

d_n of the effective Hamiltonian to be diagonalized in the P_n -space. Then, the status of a given state (model or perturber) may change along the construction of the successive model spaces (see Figure 1). However, previous inspections [35] suggest that the perturbation contribution \hat{W}_n decreases along this pre-conditioning of the Hamiltonian partitioning. Thus, the dimensions of the screened P_{n+1} -spaces should all be unity ($d_{n+1} = 1$) after the construction and diagonalization of a limited number of effective Hamiltonians. Guided by the RSBW method [35], the last step consists in a state-specific BW expansion of the energies, with well-tempered perturbation contributions (see right part in Figure 1).

To conclude this section and aid the reader's comprehension of the method, Figure 1 presents a flowchart of the computational procedure, specifically illustrating the scenario where two consecutive RS treatments are applied, followed by a final BW resolution. This computational scenario will arise in the application of the method given in the next section. Additionally, note that we also provide a pseudo-code (see Algorithm 1) that details the key numerical steps of the RSBW method. In the next section, we examine the robustness of this strategy on model Hamiltonians.

3. Spectroscopy from multi-step RSBW on model Hamiltonians

The efficiency of the multi-step RSBW treatment was examined on systems ruled by parametrized Hamiltonians. These inspections allow one to vary a selection of parameters accounting for the one- and

two-electron integrals of the electronic Hamiltonian. However, the number of parameters was limited to set up intentionally non-trivial spectroscopies (quasi-degeneracies, presence of intruder states) and to highlight the important contributions in the successive partitionings of the Hamiltonian. The energy evaluations were compared to the exact diagonalization eigenvalues.

In practice, we start with a strictly degenerate model space P_1 spanned by two reference functions $|\alpha\rangle$ and $|\alpha'\rangle$ ($d_1 = 2$), in the presence of two perturbers $|\beta\rangle$ and $|\beta'\rangle$ defining the orthogonal Q_1 -space. Limiting the number of perturbers does not harm the generality and offers a playground to assess the relevance of the here-proposed approach. The unperturbed Hamiltonian energies $\langle\alpha|\hat{H}_0|\alpha\rangle = \langle\alpha'|\hat{H}_0|\alpha'\rangle$ were set to zero, and $\langle\beta|\hat{H}_0|\beta\rangle = U$ and $\langle\beta'|\hat{H}_0|\beta'\rangle = U'$ are the positive energies of the perturbers (*e.g.* charge transfer state energies). Then, the perturbation was introduced by switching on intra and inter-space couplings. Standard notations of molecular magnetism and Hubbard model were used with $\langle\alpha|\hat{W}_0|\alpha'\rangle = K_\alpha$, $\langle\beta|\hat{W}_0|\beta'\rangle = K_\beta$, while the number of parameters for the inter-space couplings was limited with $\langle\alpha|\hat{W}_0|\beta\rangle = \langle\alpha|\hat{W}_0|\beta'\rangle = t$ and $\langle\alpha'|\hat{W}_0|\beta\rangle = \langle\alpha'|\hat{W}_0|\beta'\rangle = t'$. Note that we will consider t as the energy unit throughout the numerical inspections. The matrix structure of the

Algorithm 1 multi-step RSBW method

```

1:  $\implies$  Step 1: Initialization
2: Set  $\rho_{\min} \leftarrow cst$  (e.g. 0.5)
3: Define  $\hat{H}_0$  and  $\hat{W}_0$  such that  $(H_0)_{ij} = \delta_{ij}H_{ij}$  and  $\hat{W}_0 = \hat{H} - \hat{H}_0$ 
4: Assign the eigenvectors of  $\hat{H}_0$  to  $\{|i\rangle\}$ 
5: Assign  $\mathcal{E}_i \leftarrow \langle i | \hat{H}_0 | i \rangle$ 
6:
7:  $\implies$  Step 2: Iterative RS treatment
8: Set  $n \leftarrow 1$ 
9: Set  $i \leftarrow 0$ 
10: loop over  $i$ 
11:    $P_n = \{|i\rangle\}$ 
12:    $\dim(P_n) = 1$ 
13:   loop over  $j > i$ 
14:     Assess  $\rho_{ij,n}$  based on Eq. (4)
15:     if  $\mathcal{E}_i = \mathcal{E}_j$  or  $\rho_{ij,n} > \rho_{\min}$  then
16:        $P_n += \{|j\rangle\}$ 
17:        $\dim(P_n) += 1$ 
18:     end if
19:   end loop
20:   if  $\dim(P_n) > 1$  then
21:     Build the orthogonal  $Q_n$ -space
22:     Build & diagonalize  $\hat{H}_{\text{eff},n}^{(2)}$ 
23:     Build  $\hat{H}_n^{\text{RS}}$  and  $\hat{W}_n$  following Eq. (5)
24:     Assign the eigenvectors of  $\hat{H}_n^{\text{RS}}$  to  $\{|i\rangle\}$ 
25:     Assign  $\mathcal{E}_i \leftarrow \langle i | \hat{H}_n^{\text{RS}} | i \rangle$ 
26:     Set  $n \leftarrow n + 1$ 
27:     Set  $i \leftarrow 0$ 
28:   end if
29: end loop
30:
31:  $\implies$  Step 3: Final BW treatment
32: Compute all  $E_{i,n}^{\text{RSBW}}$  following Eq. (3)
    
```

total Hamiltonian is given by:

$$\hat{H} = \begin{pmatrix} 0 & K_\alpha & t & t \\ K_\alpha & 0 & t' & t' \\ t & t' & U & K_\beta \\ t & t' & K_\beta & U' \end{pmatrix}. \quad (7)$$

Let us first qualitatively analyze the structure of the Hamiltonian. Following Bloch theory, [36] the structure of the second-order effective Hamiltonian acting in the P_1 -space is given by :

$$\hat{H}_{\text{eff},1}^{(2)} = \begin{pmatrix} -t^2(\frac{1}{U} + \frac{1}{U'}) & K_\alpha - tt'(\frac{1}{U} + \frac{1}{U'}) \\ K_\alpha - tt'(\frac{1}{U} + \frac{1}{U'}) & -t'^2(\frac{1}{U} + \frac{1}{U'}) \end{pmatrix}. \quad (8)$$

Its diagonalization gives access to the eigenenergies $E_{0,1}^{\text{RS}}$ and $E_{1,1}^{\text{RS}}$ and their corresponding eigenvectors $|\Psi_{0,1}^{\text{RS}}\rangle$ and $|\Psi_{1,1}^{\text{RS}}\rangle$. As soon as $K_\alpha \approx U$, one of the $\hat{H}_{\text{eff}}^{(2)}$

eigenvalues gets quasi-degenerate with the perturber $|\beta\rangle$ (see Figure 1, first RS treatment). Evidently, such scenario questions the relevance of a BW approach to accurately hierarchize the different states (Section 3.1). Thus, a multi-step RS treatment might be desirable to guarantee an improved BW expansion convergence of each individual energy (Section 3.2). These problematic situations can be explored by varying a single parameter K_α . The fixed parameters defining the full Hamiltonian of the system are given in Table 1.

U	U'	K_β	t'
3.0	6.0	1.5	-1.5

Table 1: Parameters defining the full Hamiltonian ruling a system initially consisting of two model configurations and two perturbors. The model space P_1 configurations energies are used as a reference. All energies are given in $|t|$ unit ($t = -1$).

The accuracy of the method is evaluated from $\Delta = \sup_{i,n} \{|E_{i,n}^{\text{RSBW}} - E_i^{\text{exact}}|\}$, where E_i^{exact} is the exact eigenenergy of the i -th eigenstate. The BW expansion was fixed to $m = 5$ (see Eq. (3)), limiting a Δ value to 0.1 (t unit). Finally, five iterations were sufficient to reach convergence in the self-consistent treatment for all the K_α values we have considered in this study.

3.1. Single-step RSBW, $n = 1$

For $\rho_{\min} \gg 1$, $d_1 = 2$ and a self-consistent BW treatment follows the diagonalization of the effective Hamiltonian built on the strictly degenerate model space P_1 . The resulting eigenstates and eigenenergies $\{E_{i,1}^{\text{RS}}\}_{i=0-3}$ are used as zeroth-order states in the BW expansion [35]. Their variations with respect to K_α are shown in Figure 2 as a function of the coupling parameter K_α .

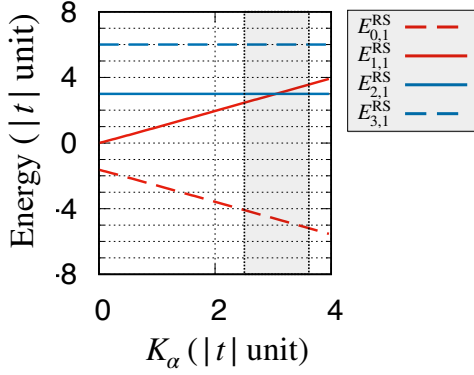


Figure 2: Variations of the two model states energies as a function of the coupling parameter K_α after the first RS treatment for $\rho_{\min} \gg 1$. The perturbers energies remain unchanged. The parameters values are given in Table 1. The critical regime is highlighted.

This preliminary inspection suggests that in the $K_\alpha \approx U$ regime, referred to as the critical regime in the following (shaded area in Figure 2), the state-specific BW procedure may lead to convergence issue due to quasi-degeneracies of the first and second excited states. Figure 3 shows the evolution of $E_{1,1}^{\text{RSBW}}$ and $E_{2,1}^{\text{RSBW}}$ as a function of K_α , featuring different behaviours.

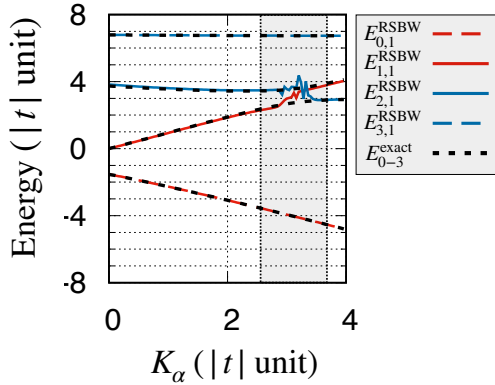


Figure 3: Approximate eigenenergies $\{E_{i,1}^{\text{RSBW}}\}_{i=0-3}$ as a function of K_α using a single-step RSBW treatment. E_{0-3}^{exact} refer to the exact energies obtained from the Hamiltonian matrix exact diagonalization.

Starting from $K_\alpha = 0$, the energies $E_{1,1}^{\text{RSBW}}$ and $E_{2,1}^{\text{RSBW}}$ obtained with a single-step RSBW treatment are in very good agreement with the exact ones. In contrast, the BW expansion breakdowns as reflected by the oscillating energies in the $K_\alpha \approx U = 3$ regime (shaded area in Figure 3). Even for $m > 5$ (see Eq. (3)), no convergence in the expansion is observed. In perturbation theory, $|\beta\rangle$ is to be considered as an intruder state for the model state spanned by $|\alpha\rangle$ and

$|\alpha'\rangle$. As expected, strongly coupled diabatic states result in the well-known avoided crossing picture. Accordingly, the wavefunctions nature changes in the vicinity of this point. Whereas the first excited state $|\Psi_1^{\text{RS}}\rangle$ is initially dominated by its projection onto $|\alpha\rangle$ and $|\alpha'\rangle$ (*i.e.* P_1 -space), the $|\beta\rangle$ and $|\beta'\rangle$ (*i.e.* Q_1 -space) predominantly contribute after the crossing (see Figure 4). Evidently, such phenomenon frequently observed in physical chemistry (mixed-valence compounds, photo-chemical processes) calls for particular care in electronic structure calculations. Finally, for higher K_α values, agreement is recovered for the first and second excited states energies.

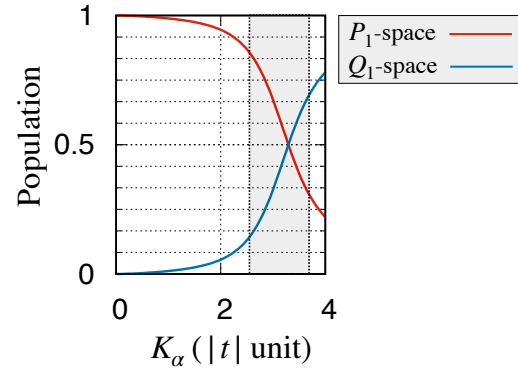


Figure 4: P_1 - and Q_1 -spaces populations of the first excited state obtained from the exact diagonalization of the \hat{H} matrix given in Eq. (7).

Despite its performance in improving perturbation approaches, the RSBW method based on a single-step RS treatment is unable to correctly describe all the eigenenergies for identified critical regimes. Thus, the next section explores a systematic way to reach a well-tempered BW energy expansion.

3.2. Multi-step RSBW approach, $n > 1$

Let us start with the zeroth-order Hamiltonian \hat{H}_1^{RS} and the perturbation $\hat{W}_1 = \hat{H} - \hat{H}_1^{\text{RS}}$. The efficiency of the BW treatment depends on the ratio ρ_{\min} introduced in Eq. (6): the larger the ρ_{\min} value, the smaller the model space size, at the cost of a slower convergence of the BW perturbative expansion. Thus, its value is to be controlled, possibly changed along the procedure to maintain tractable model space sizes. Figure 5 shows the $\rho_{ij,2}$ values calculated after the first RS step as a function of K_α .

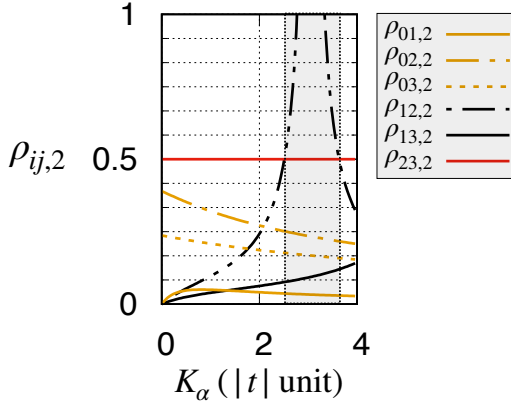


Figure 5: $\rho_{ij,2}$ values (see Eq. (6) for $n = 1$) after the first RS step as a function of K_α . The shaded area shows the critical regime defined by the criterion $\sup\{\rho_{ij,2}\} > \rho_{\min}$ where an arbitrary $\rho_{\min} = 0.5$ is used to build the P_2 model space. Note that $\rho_{23,2} = \left| \frac{K_\beta}{U' - U} \right|$ remains constant whatever K_α .

As expected from the previous discussion, a divergence in $\rho_{12,2}$ is observed for $K_\alpha \approx U = 3$. In the critical regime defined by an arbitrary $\rho_{\min} = 0.5$ (shaded area in Figure 5), a single model space P_2 is identified with $d_2 = 2$, spanned by the $|\Psi_{1,1}^{\text{RS}}\rangle$ and $|\Psi_{2,1}^{\text{RS}}\rangle$ states.

Thus, a second RS treatment must be performed to account for this strong mixing marked by the $\rho_{12,2}$ value. Since the zeroth-order energies $E_{1,1}^{\text{RS}} = \langle \Psi_{1,1}^{\text{RS}} | \hat{H}_1^{\text{RS}} | \Psi_{1,1}^{\text{RS}} \rangle$ and $E_{2,1}^{\text{RS}} = \langle \Psi_{2,1}^{\text{RS}} | \hat{H}_1^{\text{RS}} | \Psi_{2,1}^{\text{RS}} \rangle$ may differ, the updated second-order effective Hamiltonian $\hat{H}_{\text{eff},2}^{(2)}$ might not be hermitian. To remedy this possible difficulty, a common value $(E_{1,1}^{\text{RS}} + E_{2,1}^{\text{RS}})/2$ was used and the perturbation \hat{W}_2 was defined accordingly $\hat{W}_2 = \hat{H} - \hat{H}_2^{\text{RS}}$ (see Eq. (2)). At this stage, let us stress that the Q_2 -space is spanned by the ground and third excited states, $|\Psi_{0,1}^{\text{RS}}\rangle$ and $|\Psi_{3,1}^{\text{RS}}\rangle$ (see Figure 1). It is a rather unusual picture since all perturbors traditionally lie higher in energy.

For $\rho_{12,2} > \rho_{\min}$, the diagonalization of the effective Hamiltonian $\hat{H}_{\text{eff},2}^{(2)}$ defined in the P_2 -space gives access to the new zeroth-order eigenenergies $E_{1,2}^{\text{RS}}$ and $E_{2,2}^{\text{RS}}$ and their corresponding eigenvectors $|\Psi_{1,2}^{\text{RS}}\rangle$ and $|\Psi_{2,2}^{\text{RS}}\rangle$. From these quantities and \hat{W}_2 , one can easily evaluate the $\{\rho_{ij,3}\}$ values. Interestingly, by concentrating part of the perturbation in the successive redefinition of the zeroth-order Hamiltonians \hat{H}_1^{RS} and \hat{H}_2^{RS} , the ratio $\rho_{12,3}$ takes finally lower values than $\rho_{12,2}$, and even lower than $\rho_{\min} = 0.5$. Since a similar conclusion holds for all $\{\rho_{ij,3}\}$, no further RS treatment is required at this stage of the procedure.

As mentioned before, a BW expansion limited to fifth-order is conducted as the last step of the

calculation. As seen in Figure 6, agreement with exact energies ($\Delta = 0.097$) is observed in the whole range of K_α values. Let us stress that for the ground and third-excited states, this accuracy is already reached with a single-step RS and a BW expansion limited to third-order ($m = 3$). In contrast, the first and second excited states call for a multi-step RSBW approach to overcome the intruder state issue (shaded area in Figure 6) and a $m = 5$ expansion to reach the desired accuracy (i.e. $\Delta < 0.1$).

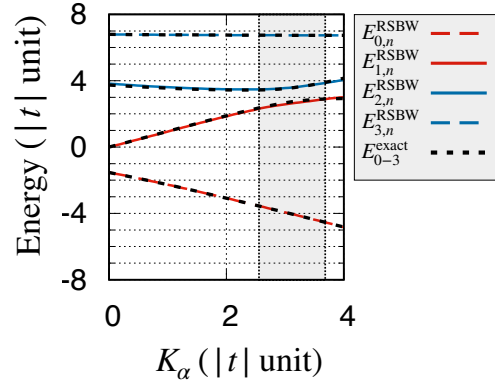


Figure 6: Approximate eigenenergies $\{E_{i,n}^{\text{RSBW}}\}_{i=0-3}$ as a function of K_α using a single- ($n=1$) or two-step ($n=2$, shaded area) RSBW treatment. E_{0-3}^{exact} refer to the exact energies obtained from the Hamiltonian matrix exact diagonalization.

The failure of the single-step RS procedure triggered by the K_α parameter is immediately identified by the divergence of $\rho_{12,1}$ (see Figure 5). Evidently, such scenario can be encountered for other sets of parameters ruling the Hamiltonian. However, the most important concern in the procedure is to check the partitioning quality $\hat{H} = \hat{H}_n^{\text{RS}} + \hat{W}_n$ after each RS step through the evaluations of the $\{\rho_{ij,n+1}\}$ ratios (see Eq. (6)). Whatever the system, the screening of interacting states can be carried out successively. As soon as $\sup\{\rho_{ij,n+1}\} < \rho_{\min}$, the subsequent BW treatment is improved, and a better description of the system's eigenenergies is guaranteed at a lower numerical cost. Along the procedure, one may at will vary the ρ_{\min} threshold to define a new critical regime and build up the associated model spaces P_n . This particular flexibility is left for future inspections.

4. Conclusion

The multi-step RSBW method we proposed combines successive Rayleigh-Schrödinger (RS) treatments leading to a well-tempered state-specific Brillouin-Wigner (BW) expansion. The strategy is to progressively include the perturbation effects by building successively

second-order effective Hamiltonians. Starting from the low-lying states, a first effective Hamiltonian is built using a first-order perturbation criterion. The resulting model functions and eigenenergies include contributions of the perturbation, and the definition of the zeroth-order Hamiltonian is revisited. Based on this updated partitioning of the Hamiltonian, the procedure is then repeated to carefully account for strongly interacting states and the presence of quasi-degeneracies.

The magnifying-glass scanning performed on subspaces not only allows one to concentrate the effort on some particular energy windows, but also to progressively reduce the impact of the resulting perturbation and the size-consistency error. Finally, a systematic and numerically cheap order-by-order BW expansion is performed on each individual state (state-specific) and leads to accurate energy transitions. The relevance of the multi-step RSBW strategy is highlighted on model Hamiltonians. The sizes of the model Hamiltonians are controlled by a threshold parameter which is to be further explored by implementing the here-proposed method on the quantum chemistry Hamiltonian.

5. Acknowledgments

This work was supported by the ANR (PRC ANR-2023-CE07-0035 AtropoPhotoCat). The authors wish to thank Prof. J. Browaeys for helpful discussions regarding accuracy assessment.

References

- [1] Yao Y and Umrigar C 2021 *Journal of Chemical Theory and Computation* **17** 4183–4194 URL <https://doi.org/10.1021/acs.jctc.1c00385>
- [2] Kossoski F, Damour Y and Loos P F 2022 *The journal of physical chemistry letters* **13** 4342–4349 URL <https://doi.org/10.1021/acs.jpcllett.2c00730>
- [3] Damour Y, Quintero-Monsebaiz R, Caffarel M, Jacquemin D, Kossoski F, Scemama A and Loos P F 2022 *Journal of Chemical Theory and Computation* **19** 221–234 URL <https://doi.org/10.1021/acs.jctc.2c01111>
- [4] Eriksen J J 2020 *The Journal of Physical Chemistry Letters* **12** 418–432 URL <https://doi.org/10.1021/acs.jpcllett.0c03225>
- [5] Garniron Y, Applencourt T, Gasperich K, Benali A, Ferté A, Paquier J, Pradines B, Assaraf R, Reinhardt P, Toulouse J et al. 2019 *Journal of chemical theory and computation* **15** 3591–3609 URL <https://doi.org/10.1021/acs.jctc.9b00176>
- [6] Coe J P 2023 *Journal of Chemical Theory and Computation* **19** 874–886 URL <https://doi.org/10.1021/acs.jctc.2c01062>
- [7] Tubman N M, Freeman C D, Levine D S, Hait D, Head-Gordon M and Whaley K B 2020 *Journal of chemical theory and computation* **16** 2139–2159 URL <https://doi.org/10.1021/acs.jctc.8b00536>
- [8] Siegbahn P, Heiberg A, Roos B and Levy B 1980 *Physica Scripta* **21** 323 URL <https://dx.doi.org/10.1088/0031-8949/21/3-4/014>
- [9] Siegbahn P E, Almlöf J, Heiberg A and Roos B O 1981 *The Journal of Chemical Physics* **74** 2384–2396 URL <https://doi.org/10.1063/1.441359>
- [10] Roos B O, Taylor P R and Siegbahn P E 1980 *Chemical Physics* **48** 157–173 URL [https://doi.org/10.1016/0301-0104\(80\)80045-0](https://doi.org/10.1016/0301-0104(80)80045-0)
- [11] Ding L, Knecht S and Schilling C 2023 *The Journal of Physical Chemistry Letters* **14** 11022–11029 URL <https://doi.org/10.1021/acs.jpcllett.3c02536>
- [12] Yalouz S, Senjean B, Günther J, Buda F, O’Brien T E and Visscher L 2021 *Quantum Science and Technology* **6** 024004 URL <https://dx.doi.org/10.1088/2058-9565/abd334>
- [13] Mizukami W, Mitarai K, Nakagawa Y O, Yamamoto T, Yan T and Ohnishi Y y 2020 *Physical Review Research* **2** 033421 URL <https://doi.org/10.1103/PhysRevResearch.2.033421>
- [14] Mahler A D and Thompson L M 2021 *The Journal of Chemical Physics* **154** URL <https://doi-org.scd-rproxy.u-strasbg.fr/10.1063/5.0053615>
- [15] Ammar A, Scemama A and Giner E 2023 *Journal of Chemical Theory and Computation* **19** 4883–4896
- [16] Yalouz S and Robert V 2023 *Journal of Chemical Theory and Computation* **19** 1388–1392 URL <https://doi.org/10.1021/acs.jctc.2c01144>
- [17] Barca G M, Gilbert A T and Gill P M 2018 *Journal of chemical theory and computation* **14** 1501–1509 URL <https://doi.org/10.1021/acs.jctc.7b00994>
- [18] Wouters S and Van Neck D 2014 *The European Physical Journal D* **68** 1–20 URL <http://dx.doi.org/10.1140/epjd/e2014-50500-1>
- [19] Keller S, Dolfi M, Troyer M and Reiher M 2015 *The Journal of chemical physics* **143** 244118 URL <https://doi.org/10.1063/1.4939000>
- [20] Liu F, Kurashige Y, Yanai T and Morokuma K 2013 *Journal of Chemical Theory and Computation* **9** 4462–4469 URL <https://doi.org/10.1021/ct400707k>
- [21] Roos B O, Linse P, Siegbahn P E and Blomberg M R 1982 *Chemical Physics* **66** 197–207 URL [https://doi.org/10.1016/0301-0104\(82\)88019-1](https://doi.org/10.1016/0301-0104(82)88019-1)
- [22] Andersson K, Malmqvist P A, Roos B O, Sadlej A J and Wolinski K 1990 *Journal of Physical Chemistry* **94** 5483–5488 URL <https://doi.org/10.1021/j100377a012>
- [23] Angeli C, Cimiraglia R, Evangelisti S, Leininger T and Malrieu J P 2001 *The Journal of Chemical Physics* **114** 10252–10264 URL <https://doi.org/10.1063/1.1361246>
- [24] Angeli C, Cimiraglia R and Malrieu J P 2001 *Chemical physics letters* **350** 297–305 URL [https://doi.org/10.1016/S0009-2614\(01\)01303-3](https://doi.org/10.1016/S0009-2614(01)01303-3)
- [25] Angeli C, Cimiraglia R and Malrieu J P 2002 *The Journal of chemical physics* **117** 9138–9153 URL <https://doi.org/10.1063/1.1515317>
- [26] Li J, Jones B A and Kais S 2023 *Science Advances* **9** eadg4576 URL <https://doi.org/10.1126/sciadv.adg4576>
- [27] Yi J and Chen F 2019 *The Journal of Chemical Physics* **150** URL <https://doi.org/10.1063/1.5081814>
- [28] Hubač I, Wilson S, Hubač I and Wilson S 2010 *Brillouin-Wigner methods for many-body systems* (Springer)
- [29] Hubač I and Neogrady P 1994 *Physical Review A* **50** 4558 URL <https://doi.org/10.1103/PhysRevA.50.4558>
- [30] Wilson S, Hubač I, Mach P, Pittner J and Čárský P 2003 *Brillouin-wigner expansions in quantum chemistry: Bloch-like and lippmann-schwinger-like equations* *Advanced Topics in Theoretical Chemical Physics* (Springer) pp 71–117

- [31] Carter-Fenk K, Shee J and Head-Gordon M 2023 The Journal of chemical physics **159**
- [32] Nesbet R 1955 Proceedings of the Royal Society of London. Series A. Mathematical and Physical Sciences **230** 312–321
- [33] Nesbet R 1955 Proceedings of the Royal Society of London. Series A. Mathematical and Physical Sciences **230** 922
- [34] Huron B, Malrieu J and Rancurel P 1973 The Journal of Chemical Physics **58** 5745–5759
- [35] Delafosse L, Hussein A, Yalouz S and Robert V 2024 Electronic Structure **6** 015009 URL <https://dx.doi.org/10.1088/2516-1075/ad28f1>
- [36] Lindgren I and Morrison J 2012 Atomic many-body theory vol 3 (Springer Science & Business Media)